维普资讯 http://www.cqvip.com



*Chinese Science Bulletin* 2006 Vol. 51 No. 11 1343—1349

DOI: 10.1007/s11434-006-1343-6

# Old EMI-type enriched mantle under the middle North China Craton as indicated by Sr and Nd isotopes of mantle xenoliths from Yangyuan, Hebei Province

MA Jinlong[1,2] & XU Yigang[1]

1. Key Laboratory of Isotope Geochronology and Geochemistry, Guangzhou Institute of Geochemistry, Chinese Academy of Sciences, Guangzhou 510640, China;
2. Graduate School of Chinese Academy of Sciences, Beijing 100039, China

Correspondence should be addressed to Xu Yigang (email: yigangxu@gig.ac.cn)

Received December 19, 2005; accepted March 21, 2006

**Abstract** Mantle xenoliths hosted in Tertiary alkali basalts in Yangyuan, Hebei Province, located to the west of the Taihangshan gravity lineament, include lherzolites, harzburgites and pyroxenite. In the plot of olivine mode *vs* Fo, most of the Yangyuan peridotites deviate from the oceanic trend, falling within the fields of Archean and Proterozoic mantles. Some LREE-enriched samples exhibit EMI-type isotopic signature with $\varepsilon_{Nd}$ ranging from –6.9 to –10.6 and $^{87}Sr/^{86}Sr$ from 0.7044 to 0.7047. By contrast, another LREE-enriched sample has a positive $\varepsilon_{Nd}$ (+5.7) similar to that for LREE-depleted peridotites. This observation suggests that the upper mantle beneath Yangyuan underwent a multi-stage metasomatism. Given the fact that EMI-type isotopic signature is usually observed in the lithosphere mantle underneath ancient cratons, the isotopic composition of the Yangyuan xenoliths provides new evidence for the existence of the old lithosphere mantle beneath western North China.

**Keywords: mantle xenoliths, Sr-Nd isotope, EMI, Yangyuan, Hebei, western North China.**

Recent studies indicate that the Mesozoic lithospheric thinning in North China was diachronous with that in west to the Taihangshan gravity lineament being later than in the eastern part of the North China Craton[1—3]. During the Cenozoic, lithospheric accretion/thickening dominated not in eastern North China but in western North China, the lithosphere is still being thinned. If the thermo-mechanical erosion is the main mechanism of lithospheric thinning[1,4], and assuming that the lithosphere protolith under North China Cration is all ancient prior to the Mesozoic, it can be inferred that the present lithosphere mantle in western China is the relics of ancient mantle, whereas that in the eastern North China Craton is a mixture of ancient mantle and newly accreted mantle[3]. Because mantle xenoliths represent the direct sample of the lithosphere mantle, they provide opportunity to testify the above-mentioned prediction. According to the plot of olivine mode *vs* olivine composition, Zheng *et al.*[5] argue that the mantle xenoliths collected from Hebi, Henan Province, located at the Daxin'anling-Taihangshan gravity lineament, have characteristics of ancient lithosphere mantle. Re-Os isotopic analyses led Gao *et al.*[6] to suggest that the peridotite xenoliths from Hannuoba (western North China) are of Archean age and peridotite xenoliths from Qixia (eastern North China) are of modern ages. Collectively, these studies imply that the region located west to the Daxin'anling-Taihang Gravity Lineament is an ideal place in searching for the relics of ancient lithosphere mantle beneath North China Craton.

Major, trace element abundances and Sr-Nd isotopic compositions are presented for the mantle peridotite xenoliths from Tertiary alkali basalts in Yangyuan, Hebei Province, western North China. Some samples are characterized by unusual EMI-type isotopic signature. Also, there is a correlation between $\varepsilon_{Nd}$ and equilibrium temperature. These data will be used to discuss the mantle metasomatic processes and lithospheric architecture in western North China.

## 1 Samples and analytical methods

Mantle xenoliths from Yangyuan are dominated by spinel lherzolites and spinel harzburgites with subordinate pyroxenites. The Yangyuan peridotites contain olivine (Ol, 62%—83%), orthopyroxene (Opx, 14%—30%), clinopyroxene (Cpx, 0.9%—10%) and spinel (Sp, 0.3%—2.1%). Most of xenoliths show a porphyroclastic texture, with grain size ranging from 1 mm to 4 mm. Protogranular and granular textures are uncommon in the Yangyuan samples.

Both major and trace element analyses were carried out in the Key Laboratory of Isotope Geochronology and Geochemistry, Chinese Academy of Sciences. Major elements were measured using a Varian VistaPro inductively coupled plasma-atomic emission spec-tro-

维普资讯 http://www.cqvip.com



meter (ICP-AES) with analytical precision better than 1%. Trace elements were obtained on a Perkin Elmer Elan 6000 ICP-MS with analytical precision better than 5%. Details of the analytical procedure has been described by Li *et al.*[7], Liu *et al.*[8] and Xu [9]. The isotopic analyses were performed on a Micromass Isoprobe Multi-Collector ICPMS. For Sr and Nd isotopic analyses, the sample powders were digested by mixed acid of $HNO_3$+ HF. Sr was separated on columns of special Sr resin and Nd was separated on HDEHP columns. Measured $^{87}Sr/^{86}Sr$ ratios were normalized to $^{88}Sr/^{86}Sr = 0.1194$. The international standard NBS987 and internal standard Sr-GIG were used to monitor the Sr isotope ratios during the analyses. Measured $^{143}Nd/^{144}Nd$ ratios were normalized to $^{146}Nd/^{144}Nd = 0.7219$ using international standard Jndi-1 and internal standard Nd-GIG as monitor. Details of the analyses of Sr and Nd isotopic ratios can be found in refs. [10, 11]. The data of elemental and isotopic compositions are listed in Table 1.

Table 1 Mineral composition, equilibrium temperature and trace element concentration (μg/g) and Sr-Nd isotopic composition of clinopyroxene from the mantle xenoliths from Yangyuan

| | Lherzolite | | | | | Harzburgite | | | | |
|---|---|---|---|---|---|---|---|---|---|---|
| | YYB-3 | YYB-4 | YYB-6 | YYB-8 | YYB-10 | YYB-1 | YYB-2 | YYB-5 | YYB-7 | YYB-9 |
| OL | 57.6 | 56.9 | 58.9 | 57.8 | 60.8 | 81.3 | 64.5 | 66.9 | 71.5 | 64.8 |
| CPX | 7.0 | 6.4 | 7.1 | 6.7 | 8.4 | 1.2 | 1.8 | 2.1 | 0.6 | 1.4 |
| OPX | 32.9 | 35.0 | 31.1 | 31.6 | 27.5 | 16.3 | 31.4 | 29.0 | 25.7 | 31.4 |
| SP | 1.2 | 0.8 | 1.5 | 1.2 | 1.0 | 3.4 | 0.9 | 0.7 | 0.2 | 1.6 |
| T (C) [a] | 872 | 1079 | 1092 | 1022 | 1113 | 1040 | | 832 | 1103 | 983 |
| $Mg^{\#}_{ol}$ | 91.1 | 91.9 | 90.9 | 91.3 | 91.4 | 91.6 | 91.8 | 91.0 | 91.8 | 91.9 |
| $Cr^{\#}_{sp}$ | 0.18 | 0.22 | 0.15 | 0.17 | 0.19 | 0.58 | 0.31 | 0.23 | 0.36 | 0.56 |
| Sc | 75.0 | 114.5 | 55.7 | 150.1 | 53.9 | 77.8 | 73.6 | 75.9 | 63.9 | 62.3 |
| Ti | 1220 | 1759 | 2738 | 2361 | 2044 | 400 | 1086 | 1733 | 888 | 143 |
| V | 246 | 273 | 238 | 294 | 224 | 220 | 229 | 232 | 231 | 151 |
| Cr | 5567 | 8332 | 5718 | 8994 | 6451 | 8765 | 8319 | 6769 | 9186 | 5044 |
| Co | 20.3 | 25.7 | 24.5 | 22.9 | 24.5 | 25.3 | 22.8 | 19.8 | 23.6 | 25.3 |
| Ni | 323 | 382 | 378 | 333 | 392 | 397 | 370 | 309 | 375 | 419 |
| Rb | 0.16 | 0.57 | 0.06 | 0.27 | 0.20 | 0.56 | 0.13 | 0.07 | 0.09 | 0.16 |
| Sr | 101 | 97.2 | 66.4 | 291 | 54.5 | 270 | 43.6 | 75.5 | 89.0 | 159 |
| Y | 15.5 | 17.5 | 19.2 | 25.6 | 17.3 | 5.18 | 9.03 | 11.0 | 9.99 | 1.68 |
| Zr | 41.4 | 27.7 | 33.7 | 39.1 | 22.6 | 28.1 | 16.3 | 14.8 | 19.2 | 7.22 |
| Nb | 1.05 | 1.08 | 0.48 | 3.87 | 0.94 | 2.53 | 0.50 | 0.52 | 1.00 | 1.69 |
| Ba | 2.56 | 7.22 | 1.89 | 6.14 | 2.40 | 2.87 | 1.48 | 1.08 | 5.05 | 3.80 |
| La | 6.23 | 1.41 | 1.11 | 4.50 | 0.84 | 13.7 | 0.65 | 1.53 | 1.83 | 30.1 |
| Ce | 19.1 | 4.31 | 3.91 | 9.01 | 2.55 | 30.51 | 2.05 | 4.87 | 4.82 | 33.17 |
| Pr | 2.94 | 0.79 | 0.79 | 1.29 | 0.46 | 3.80 | 0.41 | 0.86 | 0.80 | 1.86 |
| Nd | 12.67 | 4.49 | 4.59 | 6.48 | 3.07 | 15.09 | 2.49 | 4.53 | 4.29 | 5.20 |
| Sm | 2.34 | 1.50 | 1.73 | 2.12 | 1.36 | 2.67 | 0.90 | 1.33 | 1.35 | 0.65 |
| Eu | 0.72 | 0.63 | 0.71 | 0.89 | 0.57 | 0.83 | 0.36 | 0.49 | 0.48 | 0.15 |
| Gd | 2.28 | 2.30 | 2.69 | 3.28 | 2.29 | 2.06 | 1.23 | 1.71 | 1.63 | 0.43 |
| Tb | 0.41 | 0.44 | 0.52 | 0.64 | 0.46 | 0.29 | 0.23 | 0.29 | 0.28 | 0.06 |
| Dy | 2.72 | 3.00 | 3.47 | 4.19 | 3.16 | 1.33 | 1.55 | 1.96 | 1.85 | 0.32 |
| Ho | 0.56 | 0.61 | 0.71 | 0.91 | 0.65 | 0.20 | 0.31 | 0.40 | 0.36 | 0.06 |
| Er | 1.58 | 1.76 | 1.99 | 2.50 | 1.81 | 0.41 | 0.86 | 1.09 | 1.01 | 0.17 |
| Tm | 0.23 | 0.26 | 0.29 | 0.38 | 0.25 | 0.05 | 0.13 | 0.17 | 0.15 | 0.03 |
| Yb | 1.57 | 1.65 | 1.88 | 2.49 | 1.64 | 0.34 | 0.88 | 1.07 | 0.95 | 0.19 |
| Lu | 0.24 | 0.25 | 0.29 | 0.39 | 0.26 | 0.05 | 0.14 | 0.18 | 0.15 | 0.03 |
| Hf | 0.64 | 1.04 | 1.36 | 1.44 | 0.98 | 0.46 | 0.52 | 0.59 | 0.57 | 0.20 |
| Ta | 0.11 | 0.11 | 0.05 | 0.28 | 0.04 | 0.19 | 0.04 | 0.06 | 0.06 | 0.07 |
| Pb | 0.46 | 0.33 | 0.28 | 0.49 | 0.60 | 0.88 | 0.30 | 0.46 | 1.73 | 0.46 |
| Th | 0.16 | 0.08 | 0.04 | 0.76 | 0.09 | 1.16 | 0.05 | 0.05 | 0.11 | 8.72 |
| U | 0.05 | 0.02 | 0.01 | 0.12 | 0.02 | 0.26 | 0.01 | 0.01 | 0.03 | 1.02 |
| $^{87}Sr/^{86}Sr$ | 0.704430±15 | 0.703234±18 | 0.703266±11 | 0.704708±17 | | 0.703400±15 | | 0.704282±14 | | 0.704710±14 |
| $^{143}Nd/^{144}Nd$ | 0.512077±9 | 0.513019±13 | 0.513102±14 | 0.513056±10 | | 0.512910±9 | | 0.512695±10 | | 0.512260±13 |
| $^{87}Sr/^{86}Sr$ ($t$) | 0.704435 | 0.703227 | 0.703265 | 0.704707 | | 0.703398 | | 0.704281 | | 0.704708 |
| $\varepsilon_{Nd}$ ($t$) | −10.63 | 7.41 | 8.94 | 8.14 | | 5.65 | | 1.18 | | −6.91 |

a) Equilibration temperature is calculated using the Ca-in Opx thermometer from ref. [12].

维普资讯 http://www.cqvip.com



## 2 Results

$Al_2O_3$, CaO, $Na_2O$, $TiO_2$ contents in the Yangyuan peridotites are negatively correlated with MgO. These correlations resemble those of the world-wide peridotites, suggesting that the major compositions of the Yangyuan peridotites are mainly controlled by partial melting processes. Harzburgites have higher MgO contents and lower $Al_2O_3$ CaO, $Na_2O$ and $TiO_2$ contents than lherzolites indicating a higher degree of partial melting for the harzburgites (Table 1). Similar compositional distinction between the lherzolites and harzburgites is also reflected in mineral chemistry. For example, $Cr^{\#}$ values of Sp (0.15—0.22) in lherzolites are lower than those in harzburgites (0.23—0.58). As $Cr^{\#}_{Sp}$ is positively proportional to the degrees of partial melting, this implies that harzburgites underwent a higher degrees of melt extraction compared with lherzolites. Equilibrium temperatures for the Yangyuan peridotites, estimated using Ca-in-Opx thermobarometer of Brey *et al.*[12], range from 916°C to 1050°C. No difference in equilibrium temperature is observed between the harzburgites and lherzolites.

Fig. 1 shows the REE patterns and spider diagrams for trace elements in Cpx separates from the Yangyuan peridotites. Three REE patterns are classified. The first type is characterized by a flat HREE [$(Ho/Yb)_n$= 1.03—1.15] pattern and a LREE-depleted pattern [$(La/Yb)_n$=0.34—0.58]. Primitive mantle-normalized element abundance gradually decreases from MREE to Rb forming a smooth trend line. This pattern shows a pronounced negative Ti anomaly but no Nb and Ta-

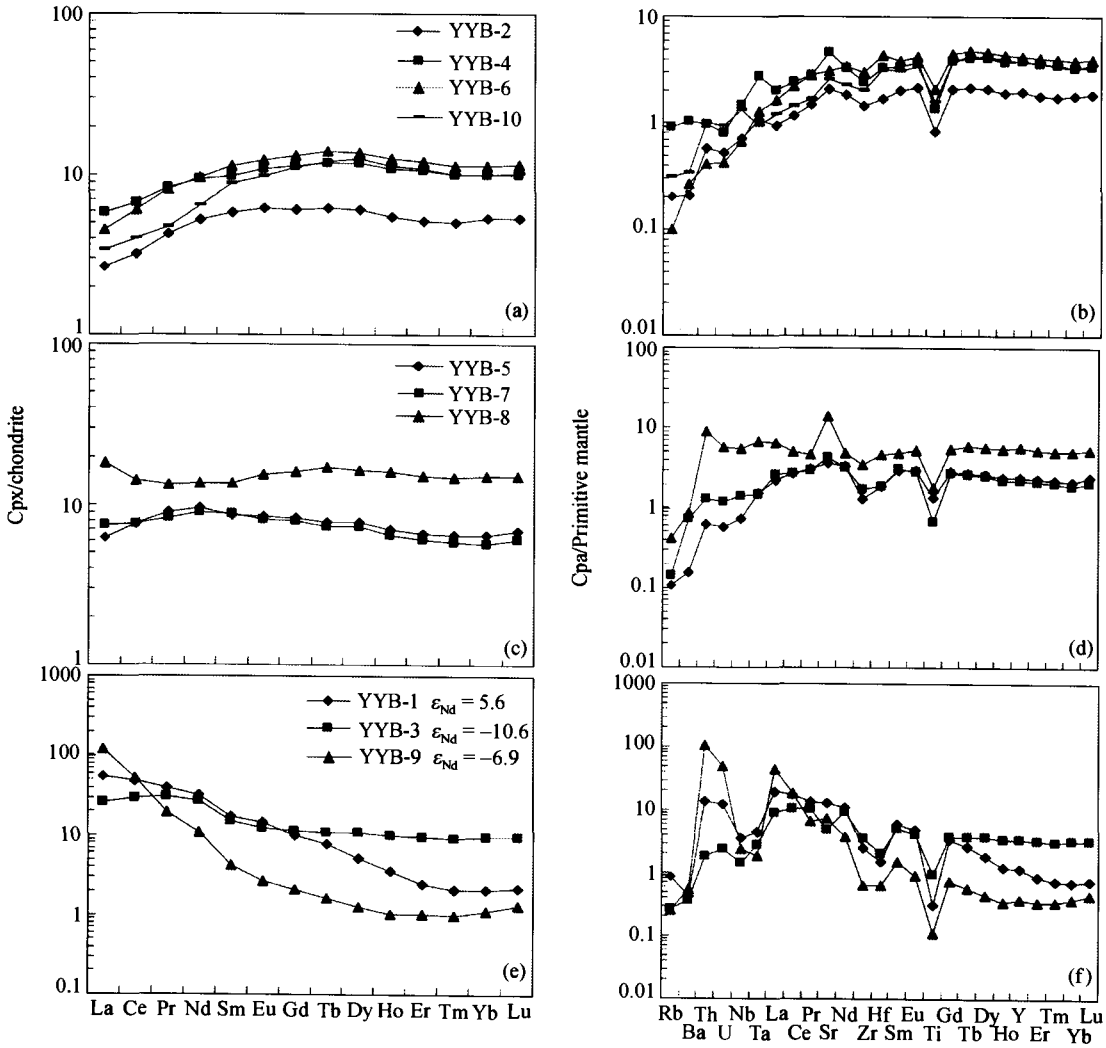


Fig. 1. REE and trace element abundances in Cpx from the Yangyuan peridotites (Chondrite and primitive mantle values are taken from ref. [13]).

维普资讯 http://www.cqvip.com



anomalies (Fig. 1(a), (b)). The second type pattern is characterized by LREE-depletion and a weak HREE fractionation with the apex at Nd (YYB-5, 7). The samples with this REE pattern exhibit negative Zr, Hf and Ti anomalies but no Nb and Ta anomalies (Fig. 1(c), (d)). The third type pattern is characterized by LREE-enrichment [$(La/Yb)_n$ = 2.7—110] and pronounced negative HFSE anomalies (Fig. 1(e), (f)). $^{87}Sr/^{86}Sr$ ratio of Cpx in the Yangyuan peridotites ranges from 0.7029 to 0.7047. $^{143}Nd/^{144}Nd$ ratios have a wide variation from 0.5120 to 0.5131. Such an isotopic signature is distinctly different from that of host basalts (Fig. 2(a)). $\varepsilon_{Nd}$ value of the LREE-enriched samples YYB-3 and YYB-9 is −10.6 and −6.9, respectively. However, their $^{87}Sr/^{86}Sr$ ratios are only moderately enriched (0.7044—0.7047), outlining an EMI-type component (Fig. 2(a)). Although YYB-1 is also LREE- enriched, it has a positive $\varepsilon_{Nd}$ value, being well within the Nd isotopic range of the LREE-depleted samples ($\varepsilon_{Nd}$ = 5—8). The $\varepsilon_{Nd}$ values of the samples with second type of REE pattern ($\varepsilon_{Nd}$ = 1.2) are between those of LREE-depleted and of the above LREE-enriched samples. There is a positive correlation between Zr content in Cpx and $\varepsilon_{Nd}$ for the Yangyuan samples except for YYB-3 (Fig. 2(b)).

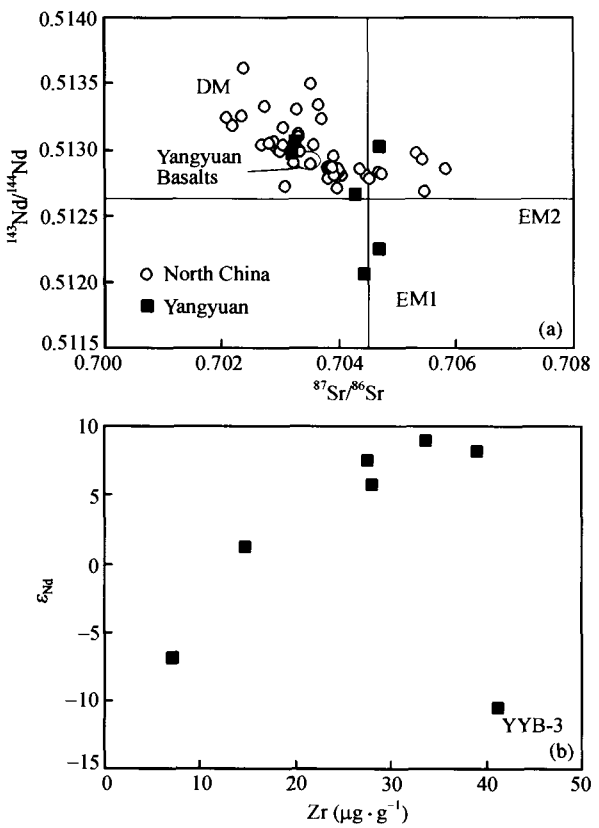


Fig. 2. (a) $^{87}Sr/^{86}Sr$ against $^{143}Nd/^{144}Nd$ in cpx; (b) Zr *vs* $\varepsilon_{Nd}$ in cpx (DM, EMI and EMII are from ref. [14], data of xenoliths from North China from refs. [15—17] and data of host basalts from ref. [18]).

## 3 Discussion

### 3.1 *Partial melting*

The negative correlation between MgO and CaO, $Al_2O_3$ contents and positive correlation between MgO and Ni and Co contents in the Yangyuan peridotite xenoliths mirror those observed for the peridotite xenoliths in Cenozoic basalts from eastern China, and can be interpreted as mantle residues of partial melting. As for the petrogenesis of harzburgites, basaltic melt-rock interaction has also been invoked in addition to melting residue model[19]. Because the typical features of melt-rock reaction such as excess opx, low $Mg^{\#}$ and flat patterns of REE[19,20] are not observed in the Yangyuan harzburgites, we thus conclude that the major element variations in the Yangyuan peridotites are mainly controlled by partial melting. Data of lherzolites and harzburgites fall along the partial melting trend calculated using fractionation melting model within the spinel stability field (Fig. 3). The degree of partial melting for lherzolites is less than 5% and 7%—20% for harzburgites.

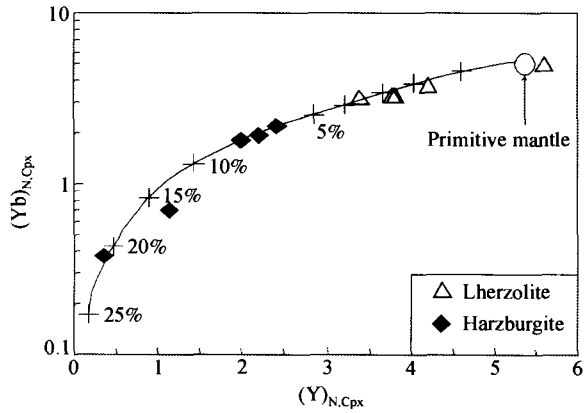


Fig. 3. Comparison of Y and Yb contents of clinopyroxenes in peridotite xenoliths from Yangyuan with the calculated melting trend using fractional melting model within spinel stability field. (Melting model and REE coefficient are from ref. [21]. Primitive mantle data are after ref. [13].)

### 3.2 *Multi-stage metasomatism*

LREE-enrichment in some Yangyuan samples suggests metasomatism in the upper mantle under this region. HREE in cpx of most samples displays a flat REE pattern, irrespective of variation of LREE contents.

维普资讯 http://www.cqvip.com



This suggests that HREE remain intact during metasomatism, consistent with the chromatographic model[22]. YYB-3 and YYB-9, which are enriched in LREE but depleted in HFSE, have negative $\varepsilon_{Nd}$ (−6.9 — −10.6) and rather limited $^{87}Sr/^{86}Sr$ variation (0.7044 — 0.7047) (Fig. 2(a)). In addition, the good positive correlation between Zr in cpx and $\varepsilon_{Nd}$ (Fig. 2(b)) can also result from mantle metasomatism. These characteristics can be explained by two alternatives: 1) Mantle metasomatism is an ancient event. Metasomatism preferentially takes place in refractory peridotites[23], consequently the more depleted samples (low Zr contents) will have lower $^{143}Nd/^{144}Nd$ ratios which resulted from the time-integrated isotopic decay from a refractory, Sm/Nd source. 2) Alternatively, metasomatism is young and low $^{143}Nd/^{144}Nd$ ratio is an intrinsic character of metasomatic agents. The positive correlation in Fig. 2(b) is the mixing line between a depleted mantle and an enriched component.

Although it is not easy to distinguish between these alternatives, we think the second alternative is unlikely because Cpx of YYB-1, which shows the trace-element pattern similar to those in YYB-3 and YYB-9 (Fig. 1(f)), has a positive $\varepsilon_{Nd}$ (+5.7). In addition, the deviation of YYB-3 deviates from the positive correlation in Fig. 3(b) is not consistent with the mixing model. On the other hand, the EMI isotopic compositions of the Yangyuan xenoliths cannot be related to subduction fluids which are characterized by high $^{87}Sr/^{86}Sr$ ratios. We thus propose that the Yangyuan LREE-enriched samples with different $\varepsilon_{Nd}$ values might reflect that the upper mantle in this region has experienced at least two-stage metasomatism, and metasomatic agent is likely the small-volume melts derived from the asthenosphere[24]. During its ascent, this melt reacted with mantle peridotites resulting in the LILE enrichment and HFSE-depletion[25] (i.e. low Sm/Nd and Rb/Sr ratios). The mantle metasomatism associated with YYB-3 and YYB-9 likely took place at an ancient time; sufficient time elapsed since the metasomatic enrichment so that low Sm/Nd and Rb/Sr ratios can translate to EMI type isotopic signature through isotopic decay. The metasomatism in YYB-1 may be a recent event. Although this sample is also characterized by low Sm/Nd and Rb/Sr ratios, the isotopic decay over a short time interval does not affect the isotopic composition of this sample. This is why YYB-1 has a depleted isotopic composition. At this stage, there is no effective method to determine the ages of metasomatic events. However, the minimum time interval of 1200 Ma between two metasomatic events in the Yangyuan mantle is required to bring the $\varepsilon_{Nd}$ value of YYB-1 to that of YYB-3. It is worth emphasizing that the conclusion about ancient mantle metasomatism is not in contradiction to the presence of ancient lithosphere mantle in this region (see the following sections).

### *3.3 Evidence for an ancient, enriched lithosphere mantle beneath Yangyuan*

Archaean, Proterozoic and Phanerozic mantle (Oceanic mantle) can be distinguished in the plot of Ol (Opx) mode against Ol composition[26,27]. Most peridotite xenoliths from Yangyuan deviate from the oceanic trend and fall within the fields of Archaean and Proterozoic mantle (Fig. 4). This is different from the oceanic trend defined by the majority of peroditite xenoliths hosted in Cenozoic basalts in eastern China[17,28]. Parallel, the EMI isotopic signature in some of the Yangyuan samples is also distinct from the predominant depleted isotopic composition in mantle xenoliths from eastern China. It is important to indicate that the mantle xenoliths with EMI isotopic compositions, which were found in kimberlite in South Africa[29] and outer hebris zone in Scotland[30], are all explained as relics of ancient lithospheric mantle. This leads us to suggest that the Yangyuan xenoliths also represent samples of the old lithosphere mantle. The presence of the late Archean lithosphere mantle under Yangyuan is also supported by low Os isotopic ratios in the same samples (mostly < 0.12 with the lowest value of 0.11; Xu *et al.*, in prep). Similar low $^{187}Os/^{188}Os$ ratios are only ob-

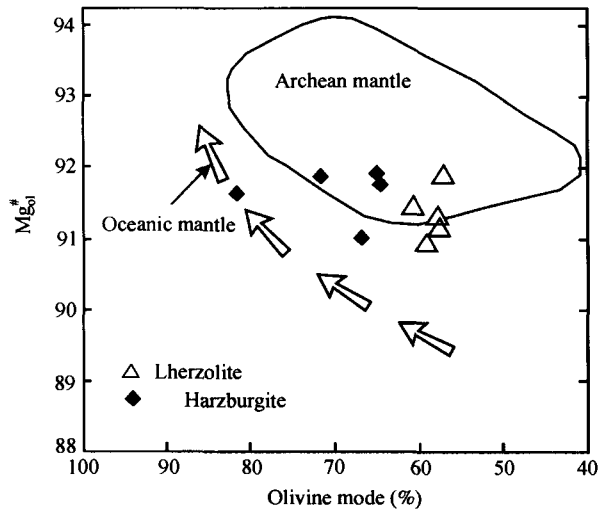


Fig. 4. Plot of Ol mode against Fo (Archaean and Proterozoic mantles and oceanic trend are from ref. [26]).

维普资讯 http://www.cqvip.com



served in the Archean cratonic peridotite xenoliths from Kaapvaal in South Africa, Siberia and Wyoming in North America[31].

Some of the Yangyuan peridotites have isotopic composition well within the MORB-OIB field. Do they represent newly accreted asthenosphere mantle? Given the following considerations, this possibility can be ruled out: (1) The newly accreted asthenosphere mantle is generally characterized by a fertile major-element composition and LREE-depleted patterns[32]. Cpx mode in the Yangyuan peridotites ranges from 8% to 0.5%, indicating a moderately to strongly refractory feature. (2) In the Shanxi basin, magmas evolved from xenolith-bearing alkali basalts of late Eocene-Oligocene age to coexisting alkali and tholeiitic basalts of late Miocene-Quaternary age. Experiments show that thoeliites originated by larger degree of partial melting at shallower depth ($15-25\times10^6$ Pa) compared with alkali basalts (> $30\times10^6$ Pa)[33]. This suggests that melting depth of asthenosphere-derived magmas gradually decreases in western North China during Cenozoic[3], consistent with the lithospheric thinning process. Accordingly there is no evidence for lithospheric accretion in this area. (3) In Fig. 4, both the samples with EMI and depleted isotopic composition deviate from the oceanic trend. Besides, there is no significant difference in Os isotopic composition between LREE-depleted and LREE-enriched samples (Xu *et al.*, in prep).

### 3.4 *Lithospheric architecture*

Fig. 5 shows that lherzolites and harzburgites have similar equilibration temperatures, but the samples with lower $\varepsilon_{Nd}$ values have lower temperatures (800—1000℃) than the samples with higher $\varepsilon_{Nd}$ (>1000℃). Although the signification of the equilibrium temperature is uncertain, it is generally accepted that they represent the *in-situ* temperature at the time of entrainment and xenoliths were equilibrated on the same conductive geotherm. Thus the observed temperature variation should reflect a variation in depth of xenolith residence[34]. Accordingly, the correlation in Fig. 5(b) may reflect lithosphere stratification with deep depleted mantle and shallow enriched mantle.

The above recognition for lithospheric architecture needs further confirmation and its formation mechanism remains uncertain. What is certain is that the lithosphere mantle at this region may not have resulted from asthenospheric accretion subsequent to lithospheric thinning, because the possibility of newly accreted asthenosphere mantle has been precluded in previous discussion. On the other hand, decompression melting during mantle upwelling will result in the negative correlation between melting degree and depth[23,35]. The lack of such correlation in the Yangyuan xenoliths probably indicates a multi-stage formation of the lithosphere mantle.

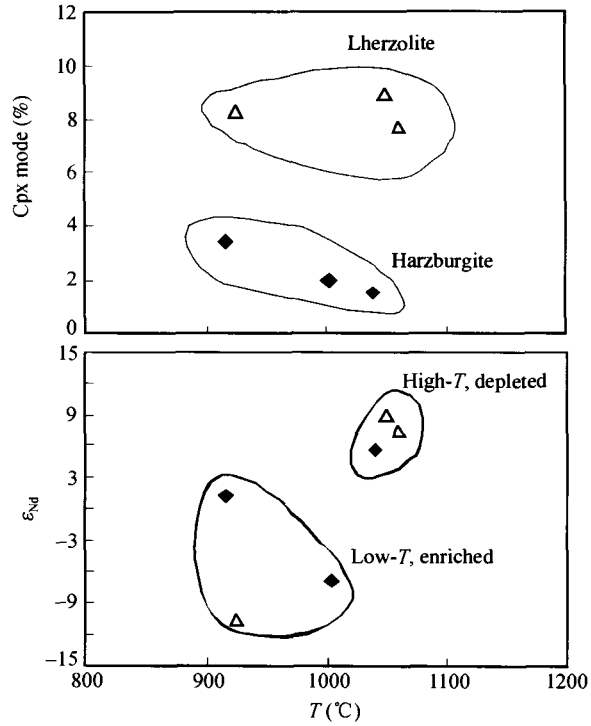


Fig. 5. (a) Equilibration temperature *vs* Cpx mode, (b) equilibration temperature *vs* $\varepsilon_{Nd}$.

**Acknowledgements** This work was supported by the Baren Project of Chinese Academy of Sciences and the National Natural Science Foundation of China (Grant No: 49925308 & 40421303).

## References

1 Griffin W L, Zhang A D, O'Reilly S Y, et al. Phanerozoic evolution of the lithosphere beneath the Sino-Korean Craton. In: Flower M, Chung S L, Lo C H, et al., eds. Mantle Dynamics and Plate Interactions in East Asia. Vol 27. Washington: Am Geophys Union Geodyn Ser, 1998. 107—126

2 Menzies M A, Xu Y G. Geodynamics of the North China Craton. In: Flower M, Chung S L, Lo C H, et al., eds. Mantle dynamics and plate interactions in east Asia. Vol 27. Washington: Am Geophys Union Geodyn Ser, 1998. 155—165

3 Xu Y G, Chung S L, Ma J L, et al. Contrasting Cenozoic lithospheric evolution and architecture in western and eastern Sino-Korean Craton: Constraints from geochemistry of basalts and man-

维普资讯 http://www.cqvip.com



tle xenoliths. J Geol, 2004, 112(5): 593－605
4 Xu Y G. Lithospheric thinning beneath North China: A temporal and spatial perspective. Geol J Chin Univ ( in Chinese), 2004, 10(3): 324－331
5 Zheng J P, O'Reilly S Y, Griffin W L, et al. Relict refractory mantle beneath the eastern North China Block: Significance for lithospheric evolution. Lithos, 2001, 57(1): 43－66
6 Gao S, Rudnick R L, Carlson R W, et al. Re-Os evidence for replacement of ancient mantle lithosphere beneath the North China Craton. Earth Planet Sci Lett, 2002, 198(3-4): 307－322
7 Li X H, Liu Y, Tu X L, et al. Precise determination of chemical compositon in silicate rocks using ICP-AES and ICP-MS: A comparative study of sample digestion techniques of alkali fusion and acid dissolution. Geochim (in Chinese), 2002, 31(3): 289－294
8 Liu Y, Liu H C, Li X H. Simultaneous and precise determination of 40 trace elements in rock sample using ICP-MS. Geochim (in Chinese), 1996, 25(6): 552－558
9 Xu Y G. Evidence for crustal components in mantle source and constraints on recycling mechanism: pyroxenite xenoliths from Hannuoba, North China. Chem Geol, 2002, 182(2-4): 301－322
10 Wei G J, Liang X R, Li X H, et al. Precise measurement of Sr isotopic composition of liquid and solid base using (LP)MC-ICPMS. Geochim (in Chinese), 2002, 31(3): 295－299
11 Liang X R, Wei G J, Li X H, et al. Fast and precise measurement for $^{143}Nd/^{144}Nd$ isotopic ratios using the Multiple-Collectors Inductively Coupled Plasma-Mass Spectrometer (MC-ICPMS). Rock and Mineral Analysis (in Chinese), 2002, 21(4): 247－251
12 Brey G G, Kohler T. Geothermobarometry in 4-phase lherzolites II: New thermobarometers, and practical assessment of existing thermobarometers. J Petrol, 1990, 31(6): 1353－1378
13 Sun S S, McDonough W F. Chemical and isotope systematics of oceanic basalts, eastern China: implications for mantle composition and process. In: Saunders A D, Norry M J, eds. Magmatism in the Ocean Basins. Vol 42. London : Geol Soc Spec, 1989. 313－345
14 Zindler A, Hart S R. Chemical geodynamics. An Rev Earth Planet Sci, 1986, 14: 493－571
15 Song Y, Frey F A. Geochemistry of peridotite xenoliths in basalt from Hannuoba, Eastern China: Implication for subcontinental mantle heterogeneity. Geochim Cosmochim Acta, 1989, 53(1): 97－113
16 Tatsumoto M, Basu A R, Hang W K, et al. Sr, Nd and Pb isotopes of ultramafic xenoliths in volcanic rocks of Eastern China: enriched components EMI and EMII in subcontinental lithosphere. Earth Planet Sci Lett, 1992, 113(1): 107－128
17 Fan W M, Zhang H F, Baker J, et al. On and off the North China craton: where is the Archaean keel ? J Petrol, 2000, 41(7): 933－950
18 Ma J L, Xu Y G. Petrology and geochemistry of the Cenozoic Basalts from Yangyuan of Hebei Province and Datong of Shanxi Province: Implications for the deep process in the Western North China Craton. Geochim (in Chinese) , 2004, 33(1): 75－88
19 Kelemen P B, Dick H J B, Quick J E. Formation of harzburgite by pervasive melt/rock reaction in the upper mantle. Nature, 1992, 358 (6388): 635－641
20 Xu Y G, Menzies M A, Thirlwall M F, et al. "Reactive" harzburgites from Huinan, NE China: products of lithosphere-asthenosphere interaction during lithospheric thinning ? Geochim Cosmochim Acta, 2003, 67(3): 487－505
21 Johnson K T M, Dick H J B, Shimizu N. Melting in the oceanic upper mantle: An ion microprobe study of diopsides in abyssal peridotite. J Geophy Res, 1990, 95(B3): 2661－2678
22 Navon O, Stolper E. Geochemical consequence of melt percolation: The upper mantle as a chromatographic column. J Geol, 1987, 95: 285－307
23 Frey F A, Green D H. The mineralogy, geochemistry and origin of lherzolite inclusions in Victorian basanites. Geochim Cosmochim Acta, 1974, 38(7): 1023－1059
24 McKenzie D P. Some remarks on the movement of small melt fractions in the mantle. Earth Planet Sci Lett, 1989, 95(1): 53－72
25 Bedini R M, Bodinier J L, Dautria J M, et al. Evolution of LILE-enriched small melt fractions in the lithospheric mantle: A case study from the Eastern African Rift. Earth Planet Sci Lett, 1997, 153(1): 67－83
26 Boyd F R. Compositional distinction between oceanic and cratonic lithosphere. Earth Planet Sci Lett, 1989, 96(1): 15－26
27 Menzies M A, Archean, Proterozoic, and Phanerozoic lithospheres. In: Menzies M A, eds. Continental mantle. London: Oxford Science Publications, 1990. 67－86
28 Xu Y G. Thermo-tectonic destruction of the Archaean lithospheric keel beneath eastern China: evidence, timing and mechanism. Phys Chem Earth (A), 2001, 26(9-10): 747－757
29 Richardson S H, Gurney J J, Erlank A J, et al. Origin of diamonds in old enriched mantle. Nature, 1984, 310(5974): 198－202
30 Menzies M, Rogers N, Tindle A, et al. Metasomatic enrichment processes in lithospheric peridotites, an effect of asthenosphere-lithosphere interaction. In: Menzies M, Hawkesworth C J, eds. Mantle Metasomatism. London: Academic Press, 1987. 313－361
31 Pearson D G, Canil D, Shirey S B. Mantle Samples included in volcanic rocks: xenoliths and diamonds. In: Holland H D, Turekin K K, eds. Treatise of Geochemistry. Oxford: Elsevier, 2003. 171－275
32 Stosch H G, Lugmair G W, Kovalenko V I. Spinel peridotite xenoliths from the Tariat Depression, Mongolia. II: Geochemistry and Nd and Sr isotopic composition and their implication for the evolution of the sub-continental lithosphere. Geochim Cosmochim Acta, 1986, 50(12): 2601－2614
33 Falloon T J, Green D H, Harton C J, et al. Anhydrous partial melting of a fertile and depleted peridotite from 2 to 30 kb and application to basalt petrogenesis. J Petrol, 1988, 29(6): 1257－1282
34 O'Reilly S Y, Griffin W L. 4-D lithosphere mapping: methodology and examples. Tectonophysics, 1996, 262(1): 3－18
35 Xu Y G, Sun M, Yan W, et al. Xenolith evidence for polybaric melting and stratification of the upper mantle beneath South China. J Asian Earth Sci, 2002, 20(8): 937－954